Uptake of chloride and iso-saccharinic acid by cement: Sorption and molecular dynamics studies on HCP (CEM I) and C-S-H phases

Yongheum Jo [a,*], Iuliia Androniuk [a], Neşe Çevirim-Papaioannou [a], Benny de Blochouse [b], Marcus Altmaier [a], Xavier Gaona [a,*]

[a] Institute for Nuclear Waste Disposal (INE), Karlsruhe Institute of Technology (KIT), Karlsruhe, Germany
[b] ONDRAF/NIRAS, Sint-Joost-ten-Node, Belgium

Keywords:
Cement
Sorption
Chloride
ISA
MD simulation

A B S T R A C T

The uptake of chloride and ISA by cement in the degradation stage I was investigated with a combination of sorption experiments and MD simulations. The retention of ^{36}Cl decreases with increasing $[Cl^-]_{tot}$ in cement pore water. The uptake of ^{36}Cl is dominated by sorption phenomena and the formation of the Friedel's salt at low and high $[Cl^-]_{tot}$, respectively. ISA sorbs moderately on HCP, and a one-site Langmuir isotherm was used to satisfactorily model the sorption data. MD simulations highlight the key role of Ca in the binding of ISA to C-S-H. This work provides a sound basis for predicting the uptake of chloride and ISA by HCP in the context of L/ILW repositories, together with new insights for the mechanistic understanding of ISA uptake.

1. Introduction

Cementitious materials are ubiquitous in repositories for low- and intermediate-level radioactive waste (L/ILW), where they are used as structural materials and for the stabilization/solidification of the waste [1]. Besides their structural functionality in the engineered barrier systems, cementitious materials are considered as one of the main materials providing high retention capacities for radionuclides in the near-field of a repository for L/ILW [2–4]. Hardened cement paste (HCP) shows high retention capacities for both cationic and anionic species due to the diversity of sorption sites available in the different cement phases or constituents [5].

In contact with groundwater, cement undergoes degradation with the consequent evolution of the main components/solid phases and pore water composition. Cement degradation is generally classified into three main stages characterized by a progressive decrease of the pH in the pore water. Stage I is controlled by the dissolution of Na- and K-oxo/hydroxide phases, which define pH values between ≈13.5 and ≈12.5 as well as increasing calcium concentration from 10^{-3} M to $2{\cdot}10^{-2}$ M with decreasing pH. The dissolution of portlandite, $Ca(OH)_2$, buffers the cement pore water composition in the degradation stage II, with pH ≈ 12.5 and [Ca] ≈ 0.02 M. After the complete dissolution of portlandite, the degradation stage III takes over, characterized by the incongruent dissolution of calcium silicate hydrated (C-S-H) phases. Throughout this third degradation stage, the Ca:Si ratio of C-S-H varies from ≈1.6 to ≈0.6, whilst the pH decreases from ≈ 12.5 to ≈ 10. Beyond portlandite and C-S-H phases, other less abundant components are also present in hardened cement paste (HCP), *i.e.* aluminoferrite trisulphate (AFt), aluminoferrite monosulphate (AFm), hydrogarnet, or hydrotalcite.

C-S-H phases are responsible for the main sorption properties of cement, mostly due to their large fraction in HCP and large surface area [6]. They are able to sorb both cations and anions, although the uptake mechanism is not well understood in many cases [4]. Dissolved calcium in the pore water importantly affects the surface charge of C-S-H phases, and accordingly their sorption behaviour. Hence, the surface charge increases from negative (stage I at pH ≈ 13.5) to positive (stage II at pH ≈ 12.5) values with increasing Ca concentration, whereas the sign of the surface charge is reversed from positive to negative with decreasing Ca:Si along the degradation stage III [7]. AFt and AFm phases are often described as hosts of anionic species *via* ion substitutions. For instance, ettringite (AFt: $Ca_6(Al,Fe)_2(OH)_{12}(SO_4)_3{\bullet}26H_2O$) may incorporate anionic radionuclides by the (partial) substitution of sulfate in its structure [8]. AFm phases have been described to accommodate Cl^- through the formation of a solid solution with Friedel's salt ($Ca_2(Al,Fe)(OH)_6Cl{\cdot}2H_2O$) [9–11]. Note that AFm and AFt phases are also considered as possible sink of organic ligands, *e.g.* gluconate, citrate or formate [12–16].

The isotope ^{36}Cl ($t_{1/2}$ $3.01{\cdot}10^5$ a) is produced *via* neutron

* Corresponding authors.
E-mail addresses: yongheum.jo@kit.edu (Y. Jo), xavier.gaona@kit.edu (X. Gaona).

activation of stable ^{35}Cl present as an impurity in fuel elements, cooling water, and structural materials (*e.g.* steel and concrete) in nuclear reactors [17–19]. Materials contaminated with ^{36}Cl (*e.g.* ion-exchange resins used for purification of reactor water) are accordingly disposed of in repositories for L/ILW, where retention processes are primarily controlled by the interaction with cementitious materials. The uptake of $^{36}Cl^-$ by HCP has been reported to correlate with the total concentration of stable Cl^- in the cement pore water [4], but it is also influenced by other parameters like pH, [Ca] and [SO_4^{2-}] [3,4]. Ochs and co-workers proposed the uptake of Cl^- to be controlled by surface processes and the formation of Friedel's salt at low and high total chloride concentrations, respectively [4]. Based on the partitioning of stable Cl^- and $^{36}Cl^-$ along the different degradation stages of cement, Wieland proposed that isotopic exchange is responsible for the uptake of $^{36}Cl^-$, whereas the formation of solid-solutions controls the concentration of stable Cl^- in the pore water [3]. However, less experimental efforts have been dedicated to assess/confirm the role of isotopic exchange as uptake mechanism of $^{36}Cl^-$ in cementitious systems. The literature reporting on the uptake of chloride by cementitious materials was critically evaluated in the review works of Wieland [3] and Ochs et al. [4], and only the most recent publications after 2016 are summarized in the following.

Cao and co-workers investigated the binding of chloride by cement in NaCl and NaCl-Na_2SO_4 systems [20]. The authors used a combination of surface complexation and solid solution modelling to reproduce their experimental observations. The surface complexes considered to form onto C-S-H phases were >SiOHCl$^-$ and >SiOCaCl, whereas Friedel's salt was the main compound accounting for the retention of chloride in the thermodynamic model. The authors observed a decreased retention of chloride in the presence of sulfate, both in the sorption and solubility (*i.e.* Friedel's salt) regimes. The effect of pH on the binding of chloride by Portland cement was investigated in a series of experiments in NaCl and $CaCl_2$ solutions with 0.25 M $\leq$ [Cl^-] $\leq$ 3.0 M [10]. The authors observed an increase on the binding of Cl^- when decreasing the pH from 13 to 12, following a clear decrease in the uptake below this pH, which approached 0 at pH 9. Thermodynamic calculations using CEMDATA14 [21–23] could only explain experimental data obtained in NaCl systems with [Cl^-] > 1 M, in which Friedel's salt possibly plays an important role in the binding of chloride. As acknowledged by the authors, the failure to properly reproduce experimental data is expectedly due to the absence of surface complexes with C-S-H in the modelling process. Jain and co-workers performed systematic potentiometric titrations with a Cl^- selective electrode and determined sorption isotherms in C-S-H, AFm and HCP in systems with pH 11.6, 12.6, 13.3 and 10^{-3} M $\leq$ [Cl^-] $\leq$ 5.0 M [11]. Experimental data were empirically fitted by means of Freundlich isotherms. Moreover, the uptake of Cl^- by HCP was successfully predicted using the isotherms derived for AFm and C-S-H, and considering the corresponding fraction of these phases in HCP as quantified by XRD and TGA. Ait Mouheb studied the uptake of $^{36}Cl^-$ and HTO by low-pH cement pastes (with pH 10.5–11) in the context of the CEBAMA EU project [24]. The author observed a weak sorption of the anions with comparable R_d values (0.1–0.4 L·kg^{-1} and 0.3–0.7 L·kg^{-1} for $^{36}Cl^-$ and HTO, respectively). The through-diffusion experiments by the same author showed that the retardation of Cl^- by sorption was negligible, and thus assumed R_d 0 for the interpretation of the data. Yoshida et al. investigated the uptake of chloride and calcium by C-S-H and calcium aluminate silicate hydrate (C-A-S-H) phases in solutions containing 0.5–2.0 M $CaCl_2$ [25]. A triple-layer model including the surface complex >XOCaCl was developed on the basis of potentiometric titration data, zeta potential measurements and ^{27}Al and ^{29}Si MAS NMR. This model satisfactorily explained Ca^{2+} and Cl^- sorption data, which however were obtained under boundary conditions well beyond standard cement pore water compositions. Nedyalkova et al. studied the sorption of ^{36}Cl, ^{125}I, HTO, and ^{14}C on fresh OPC as well as on OPC aged for >10 years at the Grimsel test site [26]. The authors used a combination of ^{36}Cl and stable Cl to vary the total chloride concentration between 10^{-6} and 0.1 M. The authors observed a significant decrease of the R_d values of ^{36}Cl with increasing added chloride concentration, and reported also a decrease in the distribution coefficients determined for fresh and aged OPC.

Iso-saccharinic acid (ISA, $C_6H_{12}O_6$) is a polyhydroxocarboxylic acid identified as main degradation product of cellulose in hyperalkaline systems containing Ca [27,28]. ISA has been reported to form strong complexes with radionuclides, including actinides, fission and activation products [29–37]. The possible formation of ISA in cellulose-containing L/ILW may enhance radionuclide solubility and decrease sorption, and thus has been focus of dedicated research in the context of nuclear waste disposal. This requires also an accurate knowledge of the concentration of ISA available in cementitious systems for complexation with the radionuclides. Although the total inventory of ISA in some specific repository packages can be very high assuming the complete degradation of cellulose (up to 1 M, see [38]), upper concentration limits are indeed set by the solubility of $Ca(ISA)_2$(cr), which defines $[ISA]_{aq} \leq$ 0.1 M (depending upon pH and [Ca]) [27,38]. Moreover, sorption studies with ISA and cement have shown a significant uptake of this organic ligand by HCP, with reported distribution coefficients (R_d, in L·kg^{-1}) ranging from 0.2 to 100. Extrapolation of these values to solid-to-liquid ratios expected under repository conditions results in significantly decreased ISA concentrations in the pore water, *i.e.* $3{\cdot}10^{-6}$ M $\leq$ [ISA] $\leq 1.9{\cdot}10^{-3}$ M [2,38].

Several studies available in the literature have investigated the uptake of ISA by C-S-H phases and HCP in different degradation stages [39–42]. These studies report a moderate sorption, which is not consistent with the electrostatic repulsion expected between ISA and the negatively charged cement/C-S-H surface in the degradation stages I and III. Van Loon, Glaus and co-workers used two-sites Langmuir isotherms to fit the sorption data of ISA and gluconate by HCP in the degradation stage I [39,43]. The derived isotherms satisfactorily explain the experimental observations under these specific boundary conditions, but do not provide insights on the mechanism/s driving the uptake of these organic ligands by HCP. Based on a series of sorption experiments with 11.6 < pH < 13.3 representing different degradation stages of cement, Pointeau and co-workers evaluated two surface complexation models to explain the uptake of ISA by C-S-H phases and HCP [40]. The fitting with the model including a mixed surface complex with Ca (>surface-Ca-ISA) showed the best agreement with experimental data, and was able to explain the stronger sorption observed for the degradation stage II. This observation correlates also with the most positive surface charge experimentally determined for the cement in this degradation stage. Two recent publications have investigated the uptake of ISA by C-S-H, CEM V (deg. stages I and II) and CEM I (deg. stage I) [41,42]. García and co-workers properly explained their sorption data of ISA onto C-S-H phases with a one-site Langmuir isotherm, while significant deviations were observed in the case of CEM V at low [ISA] [41]. On the other hand, Tasi et al. modelled the sorption of ISA by CEM I in the degradation stage II using a two-site Langmuir isotherm [42]. The slight differences observed with the capacity (q_n) and adsorption affinity constants (K_n) reported by Van Loon and co-workers can be possibly explained on the basis of the different boundary conditions considered in both studies, *e.g.* pH, [Ca] or cement particle size. Differences between the modelling approaches and modelling parameters reflect the complexity of the system, and highlight the need of further research to go beyond the empirical description of these systems.

Molecular dynamics (MD) simulations are a well-developed computational technique for studying molecular-level interactions and describing the sorption mechanisms of organics in cementitious materials. The recent literature is mostly focused on revealing the interactions of C-S-H phases with polymers [44–47], and only a few studies have been dedicated to evaluate the sorption mechanisms of small organic molecules [48,49]. In combination with wet-chemistry methods, MD arises as a promising approach to gain key insights on the mechanisms driving the uptake of organic molecules by cement.

This work focuses on the uptake of the anionic species $^{36}Cl^-$ and ISA

by CEM I in the degradation stage I. These systems are of relevance in the context of nuclear waste disposal, and are investigated by systematic sorption experiments with $1.1{\cdot}10^{-4}$ M $\leq [Cl^-]_{tot} \leq$ 2.0 M and $1.0{\cdot}10^{-5}$ M $\leq$ [ISA] $\leq$ 0.1 M, respectively. In order to gain further insights on the mechanisms driving the uptake of ISA by cement, MD simulations of the system C-S-H with ISA were performed to identify the main sorption sites and surface complexes dominating in C-S-H systems with Ca:Si ratio of ≈1.5. These boundary conditions allow the quantification of the uptake of ^{36}Cl within a wide range of total chloride concentrations expected in specific waste streams in underground repositories for nuclear waste. As for ISA, the main goal of this study targets the quantification of the ligand concentration remaining in the cement pore water after sorption. This information is important to assess the complexation and possible mobilization of radionuclides caused by ISA remaining in the cement pore water after sorption. This work is embedded in a comprehensive project dedicated to assess the retention of niobium(V) in conditions relevant for L/ILW disposal, including the effect of ISA and chloride. The current study targets the binary systems cement-Cl and cement-ISA, thus providing the baseline for the interpretation of niobium(V) uptake in the ternary and quaternary systems cement-Nb(V)-Cl, cement-Nb(V)-ISA and cement-Nb(V)-Cl-ISA as reported in [50]. From a fundamental perspective, this work targets the interaction of two anionic species with cementitious materials, extending also the discussion to the possible competition of both moieties for the sorption sites of cement.

2. Materials and methods

2.1. Chemicals

All solutions used in this work were prepared with purified water (Milli-Q, Millipore, 18.2 MΩ•cm) purged with Ar gas for several hours to remove dissolved CO_2(g). All cement materials, solutions and samples were prepared and stored in Ar glove boxes ($O_2 < 1$ ppm) at T (22 ± 2) °C. NaCl, $Ca(OH)_2$, NaOH, $CaCO_3$, NaCl, Na_2SO_4 (all EMSURE ®), NaOH (Titrisol) and KOH (Titrisol) were obtained from Merck. The ^{36}Cl stock solution used in this work (369.05 kBq·g^{-1}, 0.0084 M $Na^{36}Cl$ in H_2O, carrier free) was obtained from Eckert & Ziegler Analytics. Two types of α-isosaccharino-1,4-lactone (ISA lactone) were used for the sorption experiments with ISA: synthetic material prepared by L. Van Loon and M. Glaus (PSI-LES, Switzerland), and commercial ISA lactone obtained from Interchim. The conversion of the lactone-form into the acid, linear-form of ISA takes place within a few hours in hyperalkaline systems, and was confirmed by ^1H and ^{13}C nuclear magnetic resonance spectroscopy (see details in [50]).

2.2. Preparation of HCP and cement pore water

The HCP used in this work was prepared and characterized in [50]. Briefly, a CEM I 52,5 N SR0 CE PM-CP2 NF clinker material provided by ONDRAF-NIRAS (Belgium) was hydrated with a water-to-cement ratio of 0.46. After two days of setting time, the cement paste was cured by immersing in water for approximately 2.5 months. Afterwards, the outer layer of 2 5 mm thickness of hardened cement paste was removed to exclude any altered fraction. The cement powder was obtained by grinding with manual crushing, milling with a tungsten-carbide ball, and sieving to a particle size of <63 μm. All these preparative steps were conducted under Ar atmosphere. The resulting powder was characterized by X-ray powder diffraction (XRD), scanning electron microscope and quantitative chemical analysis after alkaline fusion with KOH [50].

Cement pore water representative of cement in the degradation stage I (Young Cement pore Water with Ca, YCWCa) was prepared following a protocol modified from [51] (see [50]). The composition of YCWCa, *i.e.* pH 13.5, [Na] 0.14 M, [K] 0.37 M, [Ca] $1.4{\cdot}10^{-3}$ M, [Si] $4{\cdot}10^{-4}$ M, $[SO_4^{2-}]$ $2{\cdot}10^{-3}$ M and $[CO_3^{2-}]$ $3{\cdot}10^{-4}$ M, remained unaltered after the equilibration with HCP at solid-to-liquid ratio (S:L) 1–50 g·L^{-1}. All preparations were conducted at T (22 ± 2 °C).

2.3. Uptake of $^{36}Cl^-$ by HCP

The uptake of chloride by cement was studied within a series of batch samples. The concentration of stable Cl^- in YCWCa after equilibration with HCP at S:L 10 and 50 g·L^{-1} was quantified by ion chromatography as $1.4{\cdot}10^{-4}$ M and $1.7{\cdot}10^{-4}$ M, respectively. The measured Cl^- was considered for the calculation of the initial chloride concentration. The content of chloride in pristine HCP was not quantified but assumed to be <55 ppm, as reported in Ochs et al. [4] for CEM I.

Sorption samples with $1.8{\cdot}10^{-4}$ M $\leq [Cl^-] \leq$ 2.0 M were prepared by spiking the required volume from NaCl stock solutions of 10^{-3} M, 0.1 M, and 2.14 M. Stock solutions were prepared by dissolution of the corresponding amount of NaCl in YCWCa. Immediately after adding stable NaCl to the suspensions, the same activity of $^{36}Cl^-$ was spiked to all sorption samples, *i.e.* 1 kBq (corresponding to $1.16{\cdot}10^{-6}$ M $^{36}Cl^-$). The samples were prepared by mixing the cement powder with the NaCl solution to achieve a solid-to-liquid ratio of 50 g·L^{-1}, although additional samples with 10 and 100 g·L^{-1} were prepared for systems containing $1.5{\cdot}10^{-4}$ and 2.0 M chloride concentration, respectively. The samples were mechanically agitated, and the activity of $^{36}Cl^-$ was determined after 9, 32, and 44 days by liquid scintillation counting (LSC). Phase separation was achieved by 10 kDa ultrafiltration (2–3 nm cut-off Nanosep®, Pall Life Sciences). Filtrates were dissolved in 2% HNO_3 with a dilution factor of 2:3, and then mixed with the cocktail solution (Ultima Gold, PerkinElmer) before the LSC measurement (1220 Quantulus and Tri-Carb 3110 TR, PerkinElmer). YCWCa containing ^{40}K was measured as a blank solution, resulting in a baseline of <1% of the total ^{36}Cl activity remaining in solution after sorption. Sorption of chloride in the 10 kD filters and in the vessel walls was quantified as negligible (< 1%).

Cement samples prepared under identical experimental conditions but using only inactive Cl^- (with 10^{-4} M $\leq [Cl^-] \leq$ 2.0 M) were characterized using a Bruker D8 Advance X-Ray powder diffractometer (Cu anode) at 2θ 4–60° with incremental steps of 0.01° and a measurement time of 0.4 s per step. All preparation and experiment were conducted at T (22 ± 3 °C).

2.4. Uptake of ISA by HCP

Batch sorption experiments with ISA were performed within the concentration range $1{\cdot}10^{-5}$ M $\leq [ISA]_0 \leq$ 0.1 M. A given amount of ISA lactone was dissolved in an artificial cement pore water without Ca ([NaOH] 0.11 M, [KOH] 0.18 M) to obtain stock solutions with [ISA] 0.02 M and 1.2 M. Samples were prepared by mixing cement powder, YCWCa, and ISA stock solutions in HDPE vials (Zinsser Analytic). The dilution effect caused by the use of ISA stock solutions in the simplified cement pore water without Ca is considered negligible (< 4%). The solid-liquid ratio was set to 1 g·L^{-1} in most of the samples, except a separate series with $[ISA]_0$ 10^{-3} M and S/L 1, 2, 10, 25 and 50 g·L^{-1}. All experiments were conducted at T (22 ± 2 °C). Reference samples with YCWCa in equilibrium with HCP (S/L 1 g·L^{-1}) and absence of ISA were characterized to account for the organic content leached by cement in these conditions. Samples with YCWCa and ISA but absence of cement were prepared to exclude possible precipitation processes in the most concentrated ISA samples. No precipitation was observed within 4 weeks, which is also in line with thermodynamic calculations conducted using thermodynamic data selected in ThermoChimie for the Ca-ISA system [52].

The concentration of ISA in the supernatant solutions was quantified by non-purgeable organic carbon (NPOC) and ion chromatography (IC) measurements after contact times of up to 4 weeks. NPOC measurement were performed with an Analytik Jena multi n/c 2100 S equipment. Aliquots of 40 to 350 μL were taken from each sorption sample, filtered with syringe filters (13 mm Disposable Filter Device, 0.1 μm pore size,

Whatman™) and diluted (1:4 to 1:1200 depending on the initial concentration of ISA) with 2% ultrapure HNO_3 in glass vials (Chromacol, Thermo Scientific). The filters were washed with YCWCa solution and the corresponding samples 3 times each to minimize (NPOC) artifacts caused by the possible leaching of organics from the filter and/or sorption of ISA onto the filter.

High-pressure ion chromatography (Integrion HPIC system) equipped with eluent generation, AS-DV autosampler and an electrochemical Pulse Amperometric Detector (gold electrode with quad potential) (Thermofisher Scientific, Dionex™) was used for the quantification of ISA at SCK-CEN (Belgium). After injection using a 40 μL injection loop on a Dionex™ PA200 column (Carbopac™) at 30 °C, elution was isocratic with 40 mM KOH at 0.5 mL/min and a total elution time of 60 min. After each sample, the column was cleaned with 1 M sodium acetate, in order to elute strongly binding carbohydrates. Ion chromatography at KIT-INE (Germany) (ICS-3000, Thermofisher Scientific, Dionex™) was also employed to measure ISA concentration in the solutions (column: Dionex™ AS9-HC, eluent: sodium carbonate 6 mM, and suppressor: Dionex™ AERS carbonate 4 mm). Selectivity was checked by addition of known concentrations of a standard after each analysis and a subsequent second analysis of each sample. The detection limits of NPOC and IC (high-pressure) measurements were quantified as $2{\cdot}10^{-5}$ M and $5{\cdot}10^{-6}$ M of ISA, respectively. The impact of the organics leached by cement in the limit of quantification of ISA based on NPOC measurements is discussed in Section 3.3 (Results and Discussion).

2.5. Computational methods

Molecular dynamics was used to study the sorption of ISA on the C-S-H surface. Calculations were performed using the (001) surface of C-S-H based on the model proposed by Jamil et al. [47]. The model was initially developed from tobermorite with a natural cleavage plane (001), parallel to silicate chains and CaO-layers. Ca/Si ratio was not modelled precisely by the number of Ca and Si atoms in the system, but rather through modelling of the main features of the interface. Only silicate layers in contact with the external solution have been modified, no changes were done to the interlayer. All the surface bridging Si were removed to get the structure of C-S-H with Ca:Si > 1.4 following available experimental spectroscopy data [53,54]. The silanol groups were deprotonated, and missing Si were replaced by Ca^{2+}. The deprotonated oxygen atoms of the surface were assigned a partial charge of q_{onb} 1.3|e|, higher than the protonated ones in the standard ClayFF model [48,55].

The interfacial aqueous solution contained 10 molecules of ISA with deprotonated carboxyl groups along with ~5400 H_2O molecules, which approximately corresponds to 0.1 M ISA initial concentration. Four of the ISA molecules had an additionally deprotonated alpha-alcohol group, which is assumed to have an important role in the Ca^{2+} complexation [56]. This concentration is in line with the range of ISA concentrations used in the sorption experiments (see Section 2.4). Aqueous hydroxyl ions were added to the system to keep the total electrostatic neutrality of the model. The calculation routine details can be found in the Supplementary Data (SD 2.1). Fig. SD-1 shows a snapshot of the simulation cell considered in the MD calculations.

3. Results and discussion

3.1. Uptake of $^{36}Cl^-$ by HCP

The uptake of $^{36}Cl^-$ by HCP is represented as distribution coefficient (R_d/L·kg^{-1}), as described by Eq. (1):

$$R_d \quad \frac{[^{36}Cl]_{solid}}{[^{36}Cl]_{aq}} \quad \frac{[^{36}Cl]_0 \quad [^{36}Cl]_{aq}}{[^{36}Cl]_{aq}} \cdot \frac{V}{m} \qquad (1)$$

where $[^{36}Cl^-]_{solid}$ is the concentration of $^{36}Cl^-$ sorbed on cement (mol·kg^{-1}), $[^{36}Cl^-]_{aq}$ is the concentration of $^{36}Cl^-$ in the aqueous phase (M), $[^{36}Cl^-]_0$ is the initial concentration of $^{36}Cl^-$ in the aqueous phase (M), V is volume of solution (L), and m is the mass of cement in the sorption sample (kg).

No clear trend of the R_d values with contacting time (9, 32, and 44 days) was observed, thus indicating that the sorption of $^{36}Cl^-$ is fast and that equilibrium conditions are attained within the considered timeframe (Fig. SD-2). The sorption study by Nedyalkova and co-workers with $^{36}Cl^-$ reported also the need of 5 and 10 days to attain equilibrium conditions [26]. Accordingly, R_d values and associated uncertainties reported in the following correspond to the average and standard deviation (±σ) of the three measurements. Fig. 1 shows the values of R_d determined in this work as a function of $[Cl^-]_{tot}$ (with $[Cl^-]_{tot}$ $[^{36}Cl^-] + [^{nat}Cl^-]$) together with data available in the literature for systems at pH > 12.8 (*i.e.* relevant to the degradation stage I). Experimental conditions of the sorption studies considered in Fig. 1 are summarized in Table 1.

Consistently with literature data, the distribution ratios determined in this work decrease with increasing $[Cl^-]_{tot}$, *i.e.* from (37.5 ± 12.0) L·kg^{-1} at $[Cl^-]_{tot}$ $1.5{\cdot}10^{-4}$ M to (0.26 ± 0.08) L·kg^{-1} at $[Cl^-]_{tot}$ 2 M. The S:L ratio was found to have a negligible effect in the R_d values within the investigated conditions, *i.e.,* 10 g·L^{-1} ≤ S:L ≤ 100 g·L^{-1}. Considering the differences in the sorption studies summarized in Fig. 1 (*e.g.* type of cement, particle size, S:L ratio), these experimental results highlight that the total chloride concentration is the main parameter controlling the uptake of Cl^- by cement as pointed out in the review work by Ochs and co-workers [4]. Two main regions can be identified in the sorption data displayed in Fig. 1: a steep decrease in the R_d values (with slope ≈ 1 for log R_d *vs.* log $[Cl^-]_{tot}$) takes place at chloride concentrations below ≈ 1 mM, whereas a systematic but less pronounced decrease in R_d is observed above this chloride concentration. This change in the slope is widely attributed to a change in the mechanism driving the uptake of chloride by HCP [3,4]. Hence, for fresh HCP, the uptake of Cl^- by C-S-H phases is often proposed to be the main mechanism binding chloride at low total Cl^- concentrations, whereas the formation of Friedel's salt or solid solutions would dominate at high total Cl^- concentrations [3,4].

Ochs and co-workers argued that isotopic exchange probably plays a relevant role in the uptake of ^{36}Cl at low total concentrations of chloride, considering that all studies investigating this total concentration range were based on mixtures of ^{36}Cl and ^{nat}Cl [4]. We note that our R_d values

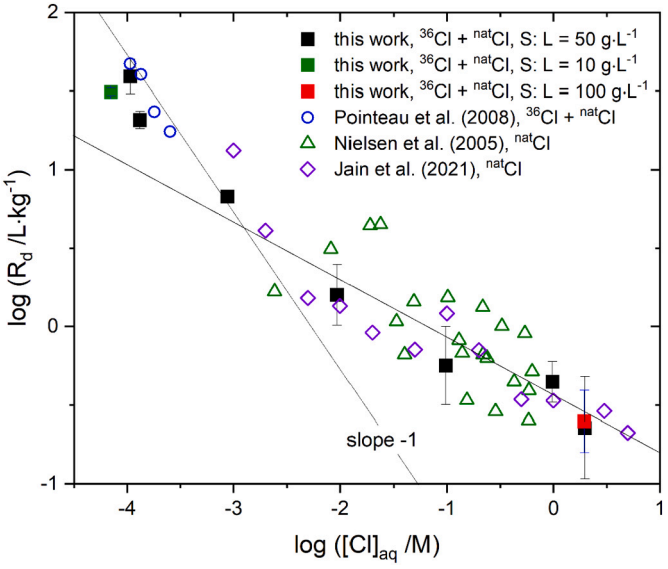

Fig. 1. Distribution coefficients (R_d) determined in this work (solid symbols) or reported in the literature (empty symbols) for the uptake of Cl by HCP in the degradation stage I (or otherwise at pH > 12.8).

Table 1
Summary of main experimental conditions in the chloride sorption experiments considered in Fig. 1 (relevant to cement degradation stage I).

Cement type	[Cl] range/M	S:L ratio/ g·L^{-1}	Contact solution	Equilibration time	R_d/ L·kg^{-1}	Reference
CEM I	1.1·10^{-4}–2.0 (^{nat}Cl) 1·10^{-6} (^{36}Cl)	10–100	YCWCa: pH 13.5, [Na] 0.14 M, [K] 0.37 M, [Ca] 1.4·10^{-3} M	44 days	0.25–37	This work
White and grey (ordinary) Portland cement	0.01–1.0 (^{nat}Cl)	660	NaOH solution: [Na] 0.25 and 0.55 M	6 months	0.3–5	[57]
CEM I	(1–3)·10^{-4} (^{nat}Cl) 7·10^{-8} (^{36}Cl)	1–7	Cement contacting water: pH 12.8–13.3	1 month	≈ 10	[40]
OPC type I	10^{-3}–5 (^{nat}Cl)	–	Synthetic PW: pH 13.3, [Na] 0.1 M, [K] 0.19 M, [Ca] 0.027 M	3 days	0.2–13	[11]

at high total chloride concentrations (determined by LSC in ^{36}Cl and ^{nat}Cl mixtures) are in good agreement with those reported by [11,57] determined exclusively using ^{nat}Cl (by potentiometry). This agreement is properly explained by the low content of chloride in cement (< 55 ppm in CEM I, as exemplarily reported in [4]), which accordingly represents only a minor fraction of the overall ^{nat}Cl inventory in the presence of high chloride concentrations in the aqueous phase. Sorption data recently reported by Nedyalkova et al. [26] for fresh OPC resulted in lower R_d values compared to other studies summarized in Fig. 1. However, chloride concentrations reported by the latter authors refer to the added and not to the total chloride concentrations, and thus measured R_d values cannot be directly compared to our experimental observations. An extended discussion on the uptake mechanism at high total chloride concentration is provided in Section 3.2, in connection with the characterization of HCP contacted with diverse NaCl concentrations.

The uptake of Cl^- by cement can be also affected by the competition with other anions present in the pore, *e.g.* OH^- or SO_4^{2-}. The addition of $CaSO_4$ and $NaSO_4$ to HCP resulted in a decreased Cl^- sorption capacity, hinting towards a competitive effect of SO_4^{2-} [58]. However, the higher content of sulfate promoted also the decrease of OH^- concentration in the pore water, and thus the impact of both parameters could not be evaluated separately. Pointeau et al. reported a decrease in the uptake of $^{36}Cl^-$ by HCP when increasing the pH of the pore water from 12.5 to 13.3 [40], although an increase in the sulfate concentration was also observed within this pH-range. We note that sorption data summarized in Fig. 1 were obtained under similar pore water conditions related to the degradation stage I [11,40,57], and thus the effect of competing ions on the uptake of chloride can be considered minor when comparing these datasets.

Fig. 2 shows the experimental sorption isotherm of Cl^- determined in this work for HCP using a combination of ^{36}Cl and ^{nat}Cl, together with sorption data reported by Jain et al. [11] under similar experimental conditions but based on experiments with ^{nat}Cl. Note that in the present work, $[Cl^-]_{solid}$ and $[Cl^-]_{aq}$ include both $^{36}Cl^-$ and $^{nat}Cl^-$, but are calculated from the quantification of ^{36}Cl in the aqueous phase and assuming the same behaviour for ^{36}Cl and ^{nat}Cl. This assumption is valid provided that the inventory of ^{nat}Cl in pristine HCP is much smaller than the total inventory of ^{nat}Cl in the system. The representation of log $[Cl^-]_{solid}$ *vs.* log $[Cl^-]_{aq}$ follows a close-to-linear trend, which can be empirically described by the Freundlich isotherm in Eq. (2):

$$log\,[Cl^-]_{solid} = n \cdot log[Cl^-]_{aq} + K_F \quad (2)$$

where n (dimensionless) and K_F ($mol^{1-n} \cdot L^n \cdot kg^{-1}$) are Freundlich constants. The fit using the Freundlich isotherm resulted in n (0.47 ± 0.03) and K_F (0.73 ± 0.13), which satisfactorily explain the complete range of chloride concentrations evaluated ($1.5 \cdot 10^{-4}$ M ≤ $[Cl^-]_{tot}$ ≤ 2.0 M). A similar outcome using the Freundlich isotherm was reported by Jain and co-workers for the uptake of chloride by HCP at pH 13.3 (dashed line in Fig. 2) [11]. The experimental conditions used by the

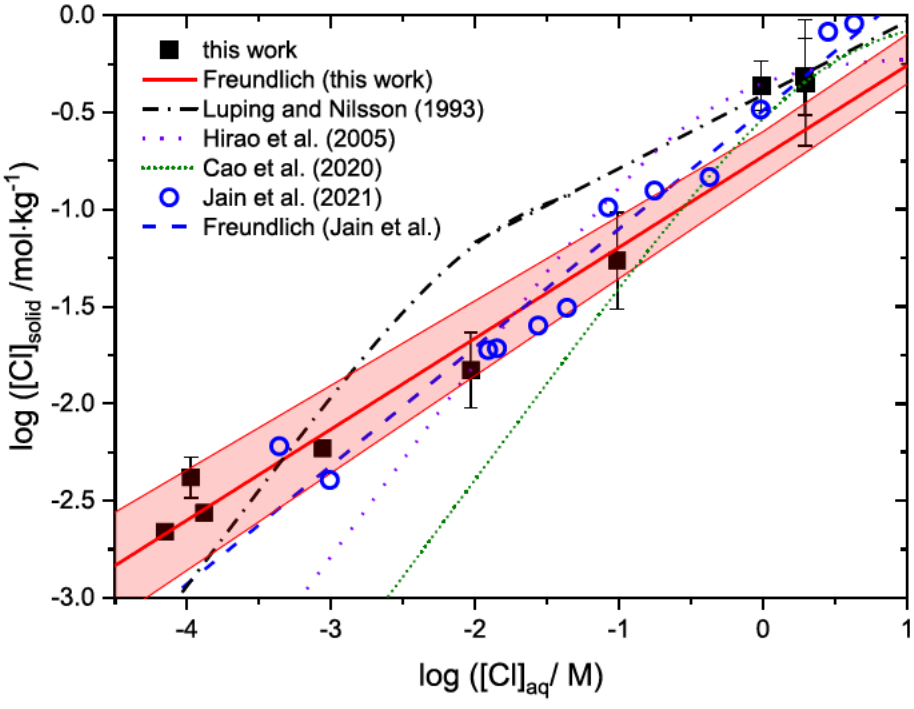

Fig. 2. Sorption of Cl as log $[Cl]_{solid}$ *vs.* log $[Cl]_{aq}$ as determined in this work (solid symbols) or reported in Jain et al. [11] (empty symbols) for CEM I in the degradation stage I. Red line and red region correspond to the Freundlich isotherm determined from experimental data in this work and corresponding uncertainty. Other lines in the figure show the sorption isotherms calculated with models/fitting parameters available in the literature [9,11,20,59] (see text for further explanations). (For interpretation of the references to colour in this figure legend, the reader is referred to the web version of this article.)

latter authors are comparable to those in the present study except for the use of ^{nat}Cl and the particle size of cement powder (20–25 μm in [11] and <63 μm in present work). The similar results obtained in both studies highlight that (i) isotopic exchange is not the main retention mechanism of ^{36}Cl within 10^{-3} M ≤ $[Cl^-]_{tot}$ ≤ 5.0 M for HCP with low chloride content in the pristine material, and (ii) the particle size of HCP does not significantly impact the uptake of Cl^-, at least below 63 μm. Point (i) can be properly rationalized considering the low inventory of ^{nat}Cl in the HCP (< 55 ppm for CEM I [4], translating to ≈<$1.5 \cdot 10^{-4}$ M in the aqueous phase assuming full dissolution and S:L 100 g·L^{-1}) and in the cement pore water with added NaCl.

Fig. 2 shows also the sorption isotherms of chloride calculated using other models and fits reported in the literature. Luping and Nilsson proposed the use of Langmuir and Freundlich isotherms for sorption data of Cl^- onto OPC paste at low (<0.05 M) and high (>0.01 M) total chloride concentrations, respectively [59]. The suggested approach compares well with our experimental data at low (<≈10^{-3} M) and high (>≈1 M) chloride concentration, but significantly deviates in the intermediate region. The model proposed by Hirao and co-workers considers also a combination of a Langmuir and Freundlich isotherms to explain the uptake of chloride by C-S-H and the formation of Friedel's salt, respectively [9]. The sorption isotherm calculated with the model by Hirao et al. agrees well with our experimental data at high chloride concentration, but importantly deviates at $[Cl^-]_{tot}$ < 0.01 M. Such disagreement is probably caused by the limited experimental data collected by the authors at low chloride concentrations and the lack of information on the uncertainties. A similar outcome is obtained using the Freundlich isotherm described by Cao and co-workers [20]. The lowest chloride concentration considered by these authors was 0.1 M, which explains the large deviations observed between their model and our experimental sorption data below this total chloride concentration.

3.2. Characterization of HCP in systems containing NaCl

The formation of Friedel's salt is considered as the main mechanism driving the uptake of Cl^- by HCP at high chloride concentrations. Because of the well-defined pattern of Friedel's salt at 2θ 11.3°, X-ray diffractograms of HCP equilibrated with YCWCa containing 0, 10^{-4}, 10^{-3}, 0.1, 1.0, and 2.0 M NaCl were collected with the aim of confirming this retention mechanism in the investigated systems. Diffractograms shown in Fig. 3 confirm that the feature of portlandite at 2θ ≈ 18° remains mostly unaltered within the complete range of NaCl concentration considered, whereas the signal corresponding to the Friedel's salt is only observed at [NaCl] ≥ 0.1 M. Previous publications have suggested that the formation of the Friedel's salt can occur even in the millimolar range of chloride concentrations [4,60], although definitive evidence is not always available for the lower range of chloride concentrations. The absence of the characteristic pattern of the Friedel's salt at [NaCl] < 0.1 M could be also explained by (i) the presence of a less crystalline form or the solid, (ii) the presence of a small fraction of the solid below the detection limit of XRD, or likely a combination of (i) and (ii). We note also that in the recent work by Jain and co-workers, the formation of the Friedel's salt was only observed at [NaCl] ≥ 0.1 M, in good agreement with data obtained in the present work [11]. The double peak at 2θ ≈ 11.3° observed in the diffractogram of HCP in 0.1 M NaCl can be assigned to the co-existence of Friedel's salt with the intermediate compound Kuzel's salt ($Ca_2Al_2(SO_4)_{0.5}Cl(OH)_{12} \cdot 6H_2O$) [61]. The phase transition from Kuzel's salt to Friedel's salt has been observed in AFm phases equilibrated with increasing NaCl concentrations [11,61].

3.3. Uptake of ISA by HCP: sorption experiments

Fig. 4 shows the comparison of ISA concentration in the sorption samples determined by NPOC and IC measurements. The figure confirms an excellent agreement between NPOC and IC results for [ISA] ≥ 10^{-5} M. The increased signal measured by NPOC at [ISA] < 10^{-5} M is

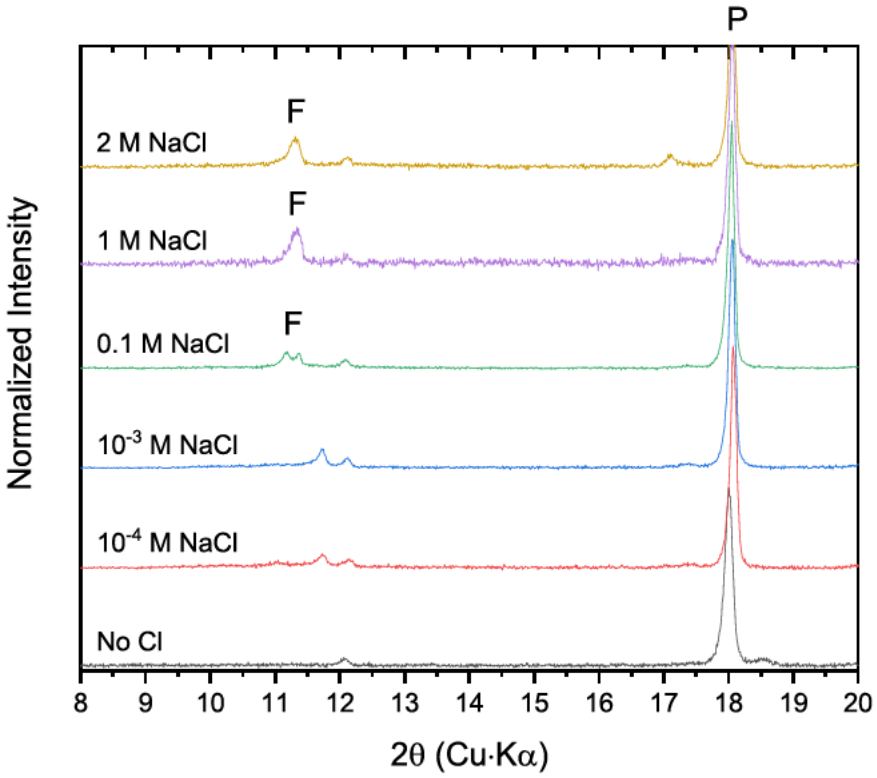

Fig. 3. XRD of HCP samples contacted with YCWCa (S:L = 1 g·L ^{1}) containing 0, 10 ^{4}, 10 ^{3}, 0.1, 1, and 2 M NaCl (F: Friedel's salt, P: portlandite). Contact time ≈ 150 days in all samples.

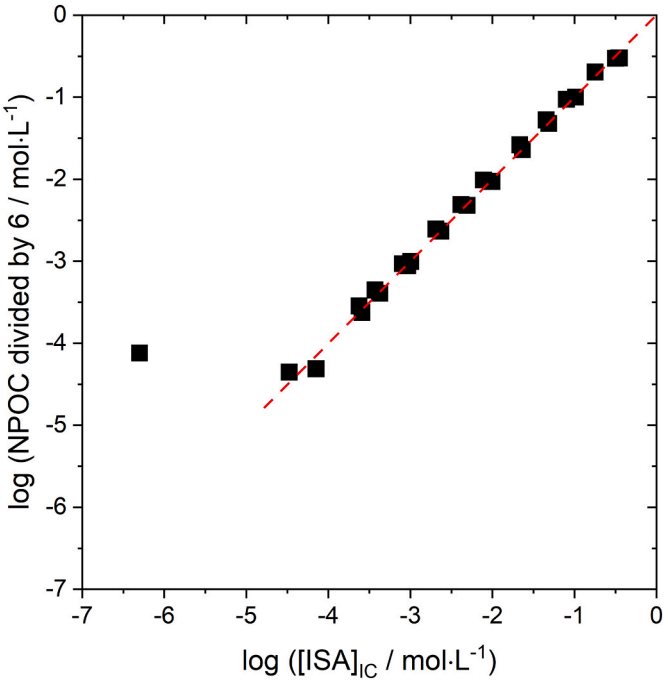

Fig. 4. Comparison of measured ISA concentrations in sorption experiments as quantified by NPOC and IC. The carbon concentration measured by NPOC was divided by 6 to obtain the concentration of ISA. Dashed line represents a slope + 1 with [NPOC]/6 = $[ISA]_{IC}$.

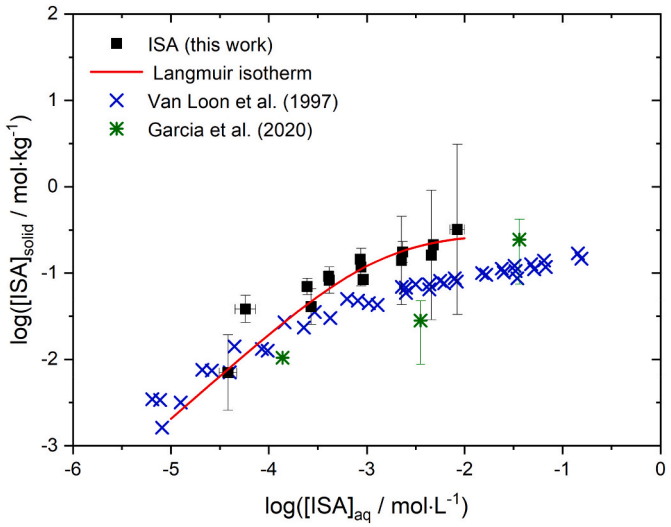

Fig. 5. Sorption isotherm of ISA on HCP equilibrated in YCWCa, with [ISA] = $10^{-4.4}$–10^{-2} M, S:L = 1 g·L^{-1}) and comparison with sorption data reported in the literature for cement systems in the degradation stage I. The line represents the one-site Langmuir model derived in this work, with K = (714 ± 266) M^{-1} and q = (0.29 ± 0.04) mol·kg^{-1}.

explained by interferences caused by the leaching of organic substances from the cement and the filter used for phase separation. The leaching was confirmed by NPOC measurements of blank samples in the absence of ISA (pore water with and without CEM I), which were quantified as $(0.6 \pm 1.3)\cdot10^{-4}$ M and $(1.1 \pm 0.1)\cdot10^{-4}$ M carbon from the cement and the filter, respectively. Due to theses interference, the sorption data obtained at [ISA] < 10^{-5} M were excluded for the data evaluation, whereas NPOC and IC results above this ligand concentration were considered as valid independent replicates of the same sorption sample. The excellent agreement between NPOC and IC results further confirms the stability of ISA against degradation within the timeframe considered in the present study (4 weeks).

The sorption isotherm of ISA on HCP equilibrated with YCWCa (degradation stage I) is shown in Fig. 5, and compared with data reported in the literature for cement systems in the same degradation stage [39,41]. Even though deprotonated anionic ISA species and negatively charged cement surface are expected at pH 13.5, the sorption of ISA on HCP is substantial and reflects slightly larger R_d values than those reported in previous studies [39–41] (see Table 2). The stronger sorption can be partially attributed to a larger surface area per unit mass of HCP caused by the smaller particle size (< 63 μm in this work), as compared to 100–400 μm in [39] or < 200 μm in [41].

Sorption data determined in this work show a similar trend as reported in [39], with a tendency to the saturation of $[ISA]_{sol}$ with increasing $[ISA]_{aq}$. Because of the lower S:L used in this work, the fraction of sorbed ISA at $[ISA]_{aq} > 10^{-3}$ M was <5% of the initial ligand concentration. Experimental error in the measurements can importantly affect sorption data at high $[ISA]_{aq}$, thus propagating a large uncertainty to $[ISA]_{sol}$. For this reason, sorption data at $[ISA]_{aq} > 10^{-2}$ M was disregarded in the data evaluation.

Sorption data at $10^{-4.4}$ M < [ISA] < 10^{-2} M was successfully fitted using a one-site Langmuir isotherm as described in Eq. (3):

$$[ISA]_{sol} \quad \frac{K \bullet q \bullet [ISA]_{aq}}{1 + K \bullet [ISA]_{aq}} \qquad (3)$$

where $[ISA]_{sol}$ is the concentration of ISA sorbed on cement (mol·kg^{-1}), K stands for the adsorption affinity constant (M^{-1}), q represents the adsorption capacity (mol·kg^{-1}), and $[ISA]_{aq}$ corresponds to the concentration of ISA in aqueous phase after sorption (M). The fit of a one-site Langmuir isotherm displayed in Fig. 5 resulted in K (714 ± 266) L·mol^{-1} and q (0.29 ± 0.04) mol·kg^{-1}. Van Loon and co-workers reported the unsuccessful description of their sorption data (with 10^{-5} M ≤ $[ISA]_{aq}$ ≤ 0.3 M) when using a one-site Langmuir isotherm [39], whereas the fit was significantly improved with a two-site Langmuir isotherm. The authors concluded that "*[…] without more information on the solid phases responsible for the sorption and the underlying adsorption mechanism(s), we see no benefit from such an exercise*". In spite of the time passed since the publication of the pioneering work by Van Loon and co-workers, definitive evidence on the underlying adsorption mechanism (s) is still missing. We note that the adsorption capacity determined in this work (q (0.29 ± 0.04) mol·kg^{-1}) is in good agreement with the sum of the concentrations of the two sorption sites defined in [39], *i.e.* q $q_1 + q_2$ (0.27 ± 0.02) mol·kg^{-1}.

García and co-workers used the one-site Langmuir isotherm to successfully describe the uptake of ISA by C-S-H phases with Ca:Si 0.8 and 1.2, whereas the same model failed to simulate the sorption of ISA on HCP in the degradation stage I (pH 13.3) and low ISA concentration, *i.e.* [ISA] ≈ 10^{-4} M [41]. The authors suggested the presence of additional sorption site(s) as a possible reason for the disagreement, but the number of data points was too limited as to draw definite conclusions on the models and sorption sites.

Independent new sorption data determined in this work at $[ISA]_0$ 10^{-3} M and 1 g·L^{-1} ≤ S:L ≤ 50 g·L^{-1} was used to validate the one-site Langmuir isotherm derived from the dataset at S:L 1 g·L^{-1} and 10^{-3} M ≤ $[ISA]_0$ ≤ 0.1 M. Hence, Fig. 6 confirms that the one-site Langmuir isotherm derived at S:L 1 g·L^{-1} can also explain the sorption behaviour of ISA at higher S:L ratios. Fig. 6 shows also that although our calculations (red solid line) predict a slightly stronger sorption than the model by Van Loon et al. [39] for HCP in the degradation stage I (blue dotted line), it represents a weaker sorption than the Langmuir isotherm derived for HCP in the degradation stage II at pH 12.5 [42]. The increased sorption at the stage II is expectedly related to the positive charge of the cement surface reported for this degradation stage of cement, which results in the electrostatic attraction of the negatively charged ISA molecule [40,42]. Indeed, Pointeau and co-workers

Table 2
Comparison of ISA sorption data on cement and experimental conditions.

Cement type/ ligand	Degradation stage/ pH	log ([ligand]$_0$/ M)	S:L/ g·L^{-1}	R_d/L·kg^{-1}	Particle size (μm)	Model and model parameters	Reference
CEM I/ISA	Stage I/13.5	−5 to −1	1	35–660	< 63	Langmuir (one-site) K (714 ± 266) L·mol^{-1} q (0.29 ± 0.04) mol·kg^{-1}	Present work
CEM I/ISA	Stage I/13.4	−5 to −0.5	25–500	1–450	100–400	Langmuir (two-sites) K_1 (1730 ± 385) L·mol^{-1} q_1 (0.1 ± 0.01) mol·kg^{-1} K_2 (12 ± 4) L·mol^{-1} q_2 (0.17 ± 0.02) mol·kg^{-1}	[27,43]
CEM I/ISA	Stage I/12.8–13.3	−3.1	1	20–80	< 50	SCM	[40]
	Stage II/12.5	−3.1	1	80		SCM	
CEM V/ISA	Stage I/13.3	−3.3 to −1.3	39	5–90	< 200	Langmuir (one-site, unsuccessful at low [ISA])	[41]
	Stage II/12.5	−3.3 to −1.3	39	15–730		Langmuir (one-site, unsuccessful at low [ISA])	
CEM I/ISA	Stage II/12.5	−3	0.2–50	64–100	< 100	Langmuir (two-sites) K_1 (2510 ± 500) L·mol^{-1} q_1 (0.18 ± 0.02) mol·kg^{-1} K_2 (12 ± 2) L·mol^{-1} q_2 (0.17 ± 0.02) mol·kg^{-1}	[42]
CEM I/GLU	Stage I/13.4	−7 to −4	17–50	0.8–1.9·10^5	< 70	Langmuir (two-sites) K_1 (2 ± 1)·10^6 L·mol^{-1} q_1 (0.04 ± 0.02) mol·kg^{-1} K_2 (2.6 ± 1.1)·10^3 L·mol^{-1} q_2 (0.7 ± 0.3) mol·kg^{-1}	[43]
CEM I/GLU	Stage II/12.5	−8 to −3	20	37–5.4·10^3	100–200	–	[62]

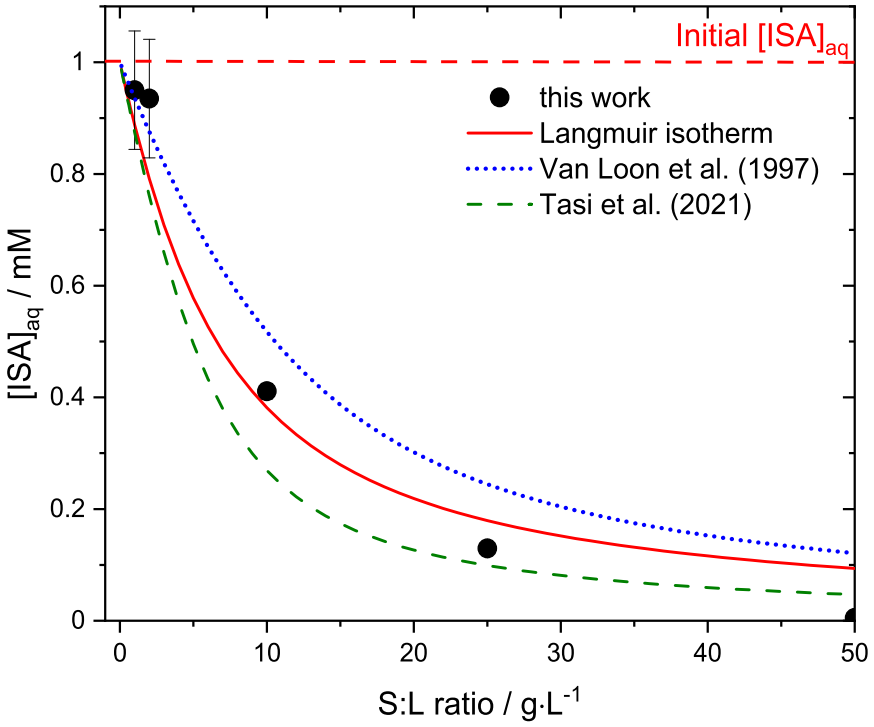

Fig. 6. ISA concentrations measured after sorption by HCP in equilibrium with YCWCa as a function of S:L ([ISA]$_0$ = 10^{-3} M, S:L = 1, 2, 10, 25, and 50 g·L^{-1}). Solid line corresponds to the calculated ISA concentrations using the one-site Langmuir isotherm derived in this work. Dotted and dashed lines show the calculated concentrations using the two-sites Langmuir isotherms described in [39] (cement degradation stage I) and [42] (cement degradation stage II), respectively.

considered surface complexation modelling to simulate the evolution of R_d as a function of pH [40]. The model assuming the formation of surface complex with a Ca-bridging (>SOCaISA) showed the best agreement with experimental sorption data, although no in-depth discussion on the proposed retention mechanistic was provided. Indeed, the key role of Ca as bridge between the surface of C-S-H and gluconate (a polyhydroxocarboxylic acid analogue of ISA) was also proposed by Androniuk and co-workers based on sorption experiments with C-S-H phases and molecular dynamics simulations [48]. Calcium was also proposed as bridge for the binding of the anionic beryllium species prevailing in hyperalkaline pH conditions (*i.e.* $Be(OH)_3^-$ and $Be(OH)_4^{2-}$) and the surface of C-S-H [63]. The role of Ca in the system C-S-H/ISA is specifically targeted in the discussion of the molecular dynamics simulations in Section 3.4.

3.4. Uptake of ISA by C-S-H phases: molecular dynamics simulations and comparison with chloride

In hyperalkaline solutions, calcium forms stable complexes with deprotonated carboxyl and the α-hydroxyl group of ISA [56]. This is confirmed by the results of classical MD of a bulk solution that can be found in the Supplementary data (Fig. SD-3).

The atomic density profiles of Ca^{2+}, aqueous hydroxyls (OHw), oxygens of hydroxyl (OH_{ISA}), and carboxyl ($O_{carb\text{-}ISA}$) functional groups of ISA in the direction perpendicular to the C-S-H surface are shown in Fig. 7a. It can be seen that both hydroxyl and carboxyl groups of ISA are found close to the surface with major peaks at the distances 0.32 and 0.57 nm for $O_{carb\text{-}ISA}$, and 0.33, 0.46, and 0.86 nm for (OH_{ISA}). No statistically significant direct coordination of ISA with silanol groups has been detected during this simulation: no density peaks closer than 0.25 nm from the surface. It can be assumed that ISA is sorbed by binding to the surface Ca^{2+} cations similar to gluconate [48]. The wide distance distribution of the density peaks shows that both inner-sphere and outer-sphere complexation is possible.

The running coordination numbers for surface Ca^{2+} and ISA oxygens have been calculated to define binding sites of organics and can be found in Fig. 7b (for the labeling of carbon atoms refer to Fig. SD-3). Because of the steric hindrance, Ca^{2+} does not bind ISA in multidentate complex [56]. Fig. 7b shows the preferable binding of Ca^{2+} to oxygens on C1, C2, C4, and C5 carbons of ISA (d 0.25 nm). Since the simultaneous coordination with four groups is not possible, two different stable complexes can be distinguished (Fig. 8): (i) coordination through carboxyl (O—C1) and α-hydroxyl group (O—C2); (ii) binding with two neighboring hydroxyl groups (O—C4 and O—C5). Finally, the hydroxyl group on C6 carbon of ISA did not participate in the complexation of Ca^{2+}. The binding sites are the same as described in the calcium isosaccharinate crystal structure [64].

The stable surface complexes of Ca^{2+} with two ISA molecules have been recorded during the production run (Fig. SD-4). This complexation was possible because of the high concentration of ISA used in the simulation model, and it does not represent the adsorption mechanism at lower concentrations.

Molecules of ISA in different protonation states have been introduced into the simulation system: with protonated and deprotonated hydroxyl groups on C2 carbon. The molecules with the deprotonated group were added together with Ca^{2+} cations, while the ones with protonated groups were not. During the simulation production, no sorption of double deprotonated ISA has been recorded. Yet two factors should be considered: the time limitation (the sorption kinetics of the neutral complex could be slower), and the force field limitation (no deprotonation possible). The hydroxyl groups of the surface complexes might get deprotonated by Ca^{2+} and this could boost the strength of binding. Nevertheless, this deprotonation should not affect the described sorption mechanisms because the Ca^{2+} polarizing abilities were partially included in the force field parameters [65].

The results of our MD calculations confirm the assumptions made by Pointeau et al. [40], who proposed a surface complex with a Ca-bridging in their surface complexation model for α-ISA sorption onto C-S-H phases to describe their experimental sorption data on fresh and degraded HCP. Pointeau and co-workers performed their experiments at constant ISA concentration ($[ISA]_0$ $8.5{\cdot}10^{-4}$ M), and thus defined the formation of only one type of surface complex, *i.e.* >SOCaISA. In contrast to this, Van Loon et al. [39] and Tasi et al. [42] reported the presence of a second sorption site to explain their experimental observations at high ISA concentrations. We speculate that the surface complex with two ISA molecules predicted in this work (see Fig. SD-4 in the Supplementary Data) may represent the second sorption site described by Van Loon et al. [39] and Tasi et al. [42], thus properly making the connection between independent experimental studies. However, the validation of this hypothesis requires extended MD simulations including dedicated efforts to calcium aluminum silicate hydrate (C-A-S-H) phases.

Chloride binding and diffusion in cementitious materials have been discussed in detail in several computational studies. The early MD studies using tobermorite and jennite structures as C-S-H proxy could not identify surface-bound chloride [66–68]. However, recent improvements in the C-S-H understanding and modelling (structure, protonation, speciation) allow a more accurate description of the uptake mechanism/s of chloride by these cement phases. Based on a combination of experimental analysis and MD simulations, Zhou and co-workers showed that Cl^- ions form more stable complexes with structural calcium of C-S-H compared to aqueous calcium [69]. The MD study by Hou et al. on Cl^- uptake by C-S-H and C-A-S-H phases confirmed that cations (Ca^{2+} and Na^+) are responsible for the sorption [70]. The recent DFT study by Svenum et al. further validated the preferential coordination of Cl^- to calcium and found that the most stable sorption sites involve at least two adjacent calcium atoms [71]. Classical MD simulations of Cl

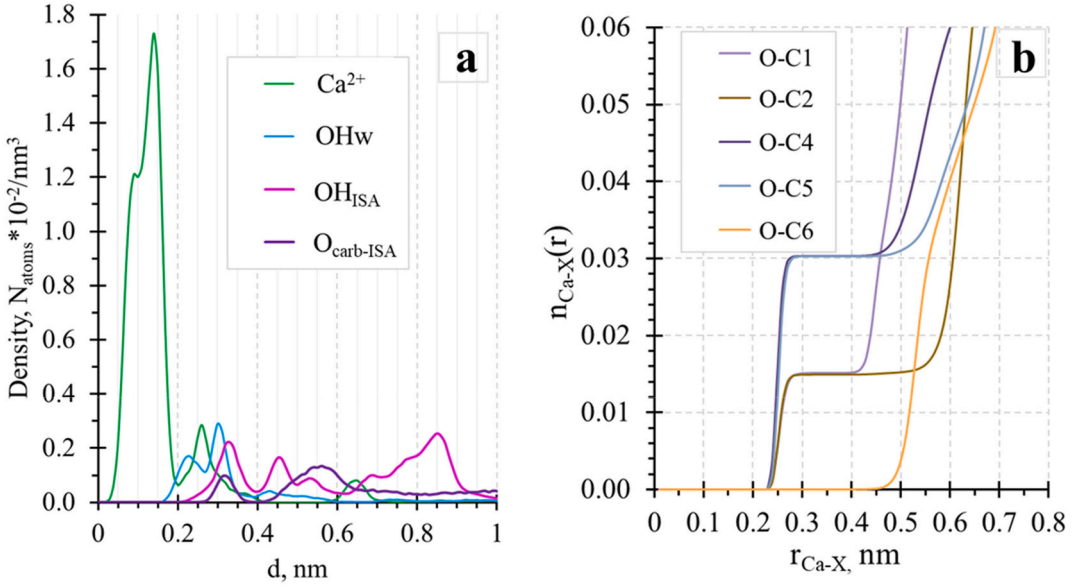

Fig. 7. (a) - Atomic density profiles of solution species near the C–S–H surface. (b) – Running coordination numbers for pairs of Ca^{2+} and different oxygens of α-ISA at the surface (d < 0.6 nm from the surface).

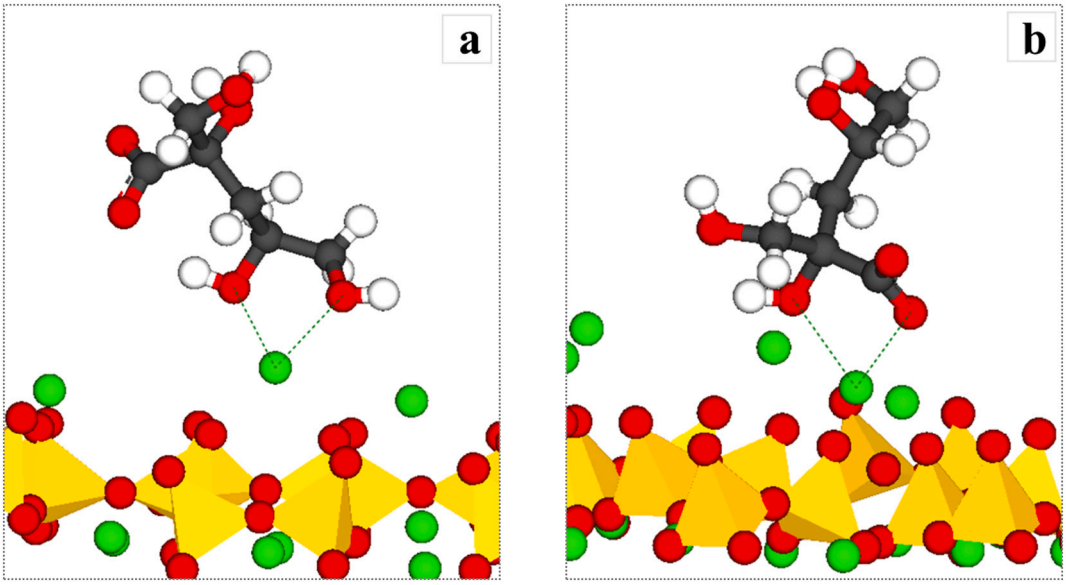

Fig. 8. The simulation snapshots of two ISA surface complexes: (a) O—C4 and O—C5 binding; (b) O—C1 and O—C2 binding (colour scheme: Si – yellow; Ca – green; O – red; H – white; C – dark grey, for the labeling of carbon atoms refer to Fig. SD-3). (For interpretation of the references to colour in this figure legend, the reader is referred to the web version of this article.)

sorption on the (001) surface of C-S-H were performed in this work for validation. The simulation details and results can be found in the Supplementary Data (SD 3.3). The results agree with the mechanism reported in the literature: Cl^- sorption on C-S-H is mediated by the surface Ca showing the same behaviour as ISA molecules. Therefore, it can be suggested that chloride will compete for the same C-S-H sorption sites with ISA. Future studies planned at KIT-INE will experimentally assess the uptake of ISA under increasing chloride concentrations to evaluate this hypothesis.

4. Conclusions

The uptake of anionic chloride and ISA by HCP (CEM I) in equilibrium with an artificial cement pore water representative of the cement degradation stage I (YCWCa) was investigated under a wide variation of the main parameters, *i.e.* $1.8{\cdot}10^{-4}$ M $\leq [Cl^-]_{tot} \leq$ 2.0 M (with constant $[^{36}Cl^-]$ $1.2{\cdot}10^{-6}$ M), 10^{-5} M $\leq [ISA]_0 \leq$ 0.1 M and 1 g·L^{-1} $\leq$ S:L $\leq$ 100 g·L^{-1}.

The concentration of stable Cl^- leached from HCP at S:L 10 and 50 g·L^{-1} was quantified as $1.4{\cdot}10^{-4}$ M and $1.7{\cdot}10^{-4}$ M, respectively. The total concentration of Cl^- in the aqueous phase significantly affected the sorption of $^{36}Cl^-$ by HCP in the degradation stage I. A clear decrease in R_d values was observed with increasing $[Cl^-]_{tot}$, from (37.5 ± 12.0) L·kg^{-1} at $[Cl^-]_{tot}$ $1.5{\cdot}10^{-4}$ M to (0.26 ± 0.08) L·kg^{-1} at $[Cl^-]_{tot}$ 2.0 M. Sorption data can be classified in two main regions: the stronger uptake observed at lower $[Cl^-]_{tot}$ ($<\approx 10^{-3}$ M) is often attributed to adsorption processes, whereas the presence of the Friedel's salt and formation of solid solutions is considered as the main mechanism driving the uptake of $^{36}Cl^-$ at high total chloride concentrations. The confirmation by XRD of the presence of the Friedel's salt at $[Cl^-]_{tot} \geq 0.1$ M underlines the latter hypothesis. The excellent agreement between R_d values and sorption isotherms obtained in this work with $^{36}Cl + {}^{nat}Cl$ and reported in the literature for ^{nat}Cl supports that isotopic exchange plays a minor role in the uptake of ^{36}Cl by CEM I in the degradation stage I at total chloride concentrations above $\approx 10^{-3}$ M. Sorption data were successfully modelled using a Freundlich isotherm. This approach properly explains experimental observations within the investigated range of chloride concentrations ($1.5{\cdot}10^{-4}$ to 2.0 M), but represents an empirical description of the system without providing any mechanistic understanding of the retention process.

Sorption experiments with ISA confirmed a moderate uptake by HCP in the degradation stage I, with R_d values ranging between 35 and 660 L·kg^{-1}. These values are slightly higher but in line with those obtained in previous studies under similar experimental conditions. Sorption data determined at S:L 1 g·L^{-1} with 10^{-5} M $\leq [ISA]_{aq} \leq 10^{-2}$ M were successfully modelled using a one-site Langmuir isotherm. An independent dataset with $[ISA]_0$ 10^{-3} M and 1 g·L^{-1} $\leq$ S:L $\leq$ 50 g·L^{-1} was used to validate the proposed Langmuir isotherm. As previously reported for the uptake of chloride and anionic beryllium species by C-S-H, MD simulations confirmed the key role of Ca as bridge between ISA and the C-S-H surface. The formation of a second surface complex hinted by MD at high ISA concentrations could be interpreted as a second sorption site in the C-S-H surface/HCP, a hypothesis proposed by other empirical models available in the literature [40]. On-going and future work at KIT-INE with MD simulations aim at a mechanistic understanding of the processes driving the uptake of organic molecules/ligands (ISA and beyond) by cement. The results of this work provide an improved bases for predicting the uptake of chloride and ISA by HCP in the context of L/ILW repositories, whilst serving as baseline for the interpretation of more complex systems involving radionuclides, *i.e.* niobium (see related paper by [50]).

CRediT authorship contribution statement

Yongheum Jo: Methodology, Investigation, Writing – original draft, Writing – review & editing. **Iuliia Androniuk:** Investigation, Writing – original draft. **Neşe Çevirim-Papaioannou:** Methodology, Investigation, Writing – review & editing. **Benny de Blochouse:** Conceptualization, Project administration, Writing – review & editing. **Marcus Altmaier:** Conceptualization, Project administration, Funding acquisition, Writing – review & editing. **Xavier Gaona:** Conceptualization, Supervision, Project administration, Funding acquisition, Writing – original draft, Writing – review & editing.

Declaration of competing interest

The authors declare that they have no known competing financial interests or personal relationships that could have appeared to influence the work reported in this paper.

Acknowledgements

This work was partly funded by ONDRAF-NIRAS. Frank Geyer, Annika Kaufmann, Stefanie Kuschel, Melanie Bottle, Jonas Rentmeister (all KIT–INE) are gratefully acknowledged for the ICP-MS/OES, IC, LSC, NPOC measurements and technical support. Luc Van Loon and Martin Glaus (PSI-LES) are kindly acknowledged for providing the α-iso-saccharino-1,4-lactone used in this study. We thank Katinka Wouters and technical staff at SCK-CEN for IC measurement. The authors acknowledge support by the state of Baden-Württemberg through bwHPC and the German Research Foundation (DFG) through grant no INST 40/575-1 FUGG (JUSTUS 2 cluster).

Appendix A. Supplementary data

Supplementary data to this article can be found online at https://doi.org/10.1016/j.cemconres.2022.106831.

References

[1] M. Atkins, F.P. Glasser, Application of Portland cement-based materials to radioactive waste immobilization, Waste Manag. 12 (1992) 105–131.
[2] E. Wieland, L.Van Loon, Cementitious Near-field Sorption Data Base for Performance Assessment of an ILW Repository in Opalinus Clay. Technical Report 03-06, Paul Scherrer Institut, Villigen, Switzerland, 2003.
[3] E. Wieland, Sorption Data Base for the Cementitious Near Field of L/ILW and ILW Repositories for Provisional Safety Analyses for SGT-E2, Nagra Technical Report 14-08, Paul Scherrer Institut, Villigen, Switzerland, 2014.
[4] M. Ochs, D. Mallants, L. Wang, Radionuclide and Metal Sorption on Cement and Concrete, Springer, Switzerland, 2016.
[5] B. Grambow, M. López-García, J. Olmeda, M. Grivé, N.C.M. Marty, S. Grangeon, F. Claret, S. Lange, G. Deissmann, M. Klinkenberg, D. Bosbach, C. Bucur, I. Florea, R. Dobrin, M. Isaacs, D. Read, J. Kittnerová, B. Drtinová, D. Vopálka, N. Cevirim-Papaioannou, N. Ait-Mouheb, X. Gaona, M. Altmaier, L. Nedyalkova, B. Lothenbach, J. Tits, C. Landesman, S. Rasamimanana, S. Ribet, Retention and diffusion of radioactive and toxic species on cementitious systems: Main outcome of the CEBAMA project, Appl. Geochem. 112 (2020), 104480.
[6] J. Tits, E. Wieland, C.J. Müller, C. Landesman, M.H. Bradbury, Strontium binding by calcium silicate hydrates, J. Colloid Interface Sci. 300 (2006) 78–87.
[7] I. Pointeau, P. Reiller, N. Macé, C. Landesman, N. Coreau, Measurement and modeling of the surface potential evolution of hydrated cement pastes as a function of degradation, J. Colloid Interface Sci. 300 (2006) 33–44.
[8] M.L.D. Gougar, B.E. Scheetz, D.M. Roy, Ettringite and C-S-H Portland cement phases for waste ion immobilization: a review, Waste Manag. 16 (1996) 295–303.
[9] H. Hirao, K. Yamada, H. Takahashi, H. Zibara, Chloride binding of cement estimated by binding isotherms of hydrates, J. Adv. Concr. Technol. 3 (2005) 77–84.
[10] P. Hemstad, A. Machner, K. De Weerdt, The effect of artificial leaching with HCl on chloride binding in ordinary Portland cement paste, Cem. Concr. Res. 130 (2020), 105976.
[11] A. Jain, B. Gencturk, M. Pirbazari, M. Dawood, A. Belarbi, M.G. Sohail, R. Kahraman, Influence of pH on chloride binding isotherms for cement paste and its components, Cem. Concr. Res. 143 (2021), 106378.
[12] A.M. Cody, H. Lee, R.D. Cody, P.G. Spry, The effects of chemical environment on the nucleation, growth, and stability of ettringite [Ca3Al(OH)6]2(SO4)3·26H2O, Cem. Concr. Res. 34 (2004) 869–881.
[13] H. Pollmann, S. Stefan, E. Stern, Synthesis, characterization and reaction behaviour of lamellar AFm phases with aliphatic sulfonate-anions, Cem. Concr. Res. 36 (2006) 2039–2048.
[14] E. Wieland, A. Jakob, J. Tits, B. Lothenbach, D. Kunz, Sorption and diffusion studies with low molecular weight organic compounds in cementitious systems, Appl. Geochem. 67 (2016) 101–117.
[15] Q. Wang, C. Taviot-Gueho, F. Leroux, K. Ballerat-Busserolles, C. Bigot, G. Renaudin, Superplasticizer to layered calcium aluminate hydrate interface characterized using model organic molecules, Cem. Concr. Res. 110 (2018) 52–69.
[16] R.E. Guidone, B. Lothenbach, X. Gaona, A. Tasi, M. Altmaier, H. Geckeis, Interaction of low molecular weight organics, cement phases and radionuclides, in: Proceedings of the European Nuclear Young Generation ForumTarragona, Spain, 2021.
[17] L. Xinqi, H.W. Gaggeler, D. Laske, H. Synal, W. Wolfli, F.C.J. Brandt, J.C. Alder, K. Kurtz, Determination of the 36cl Content in Reactor Cooling Water and Active Resins From Swiss Nuclear Power Plants, Technical Report 91 -07, Wettingen, Switzerland, 1991.
[18] S.C. Sheppard, L.H. Johnson, B.W. Goodwin, J.C. Tait, D.M. Wuschke, C. C. Davison, Chlorine-36 in nuclear waste disposal—1. Assessment results for used fuel with comparison to 129I and 14C, Waste Manag. 16 (1996) 607–614.
[19] S.J. Parry, B.A. Bennett, R. Benzing, D. Redpath, J. Harrison, P. Wood, F.J. Brown, Radiochemical neutron activation analysis for trace chlorine in steels and alloys, Anal. Chem. 69 (1997) 3049–3052.
[20] Y. Cao, L. Guo, B. Chen, J. Wu, Thermodynamic modelling and experimental investigation on chloride binding in cement exposed to chloride and chloride-sulfate solution, Constr. Build. Mater. 246 (2020), 118398.
[21] B. Lothenbach, T. Matschei, G. Moschner, F.P. Glasser, Thermodynamic modelling of the effect of temperature on the hydration and porosity of Portland cement, Cem. Concr. Res. 38 (2008) 1–18.
[22] T. Matschei, B. Lothenbach, F.P. Glasser, Thermodynamic properties of Portland cement hydrates in the system CaO–Al2O3–SiO2–CaSO4–CaCO3–H2O, Cem. Concr. Res. 37 (2007) 1379–1410.
[23] B. Lothenbach, L. Pelletier-Chaignat, F. Winnefeld, Stability in the system CaO–Al2O3–H2O, Cem. Concr. Res. 42 (2012) 1621–1634.
[24] N.Ait Mouheb, Radionuclide Migration in Low-ph Cement/Clay Interfaces: Derivation of Reactive Transport Parameters, 2020. PhD Thesis.
[25] S. Yoshida, Y. Elakneswaran, T. Nawa, Electrostatic properties of C-S–H and C-A-S-H for predicting calcium and chloride adsorption, Cem. Concr. Compos. 121 (2021), 104109.
[26] L. Nedyalkova, J. Tits, E. Bernard, E. Wieland, U. Mader, Sorption experiments with HTO, 36-cl, 125-I and 14-C labeled formate on aged cement matrices retrieved from long-term in-situ rock laboratory experiments, J. Adv. Concr. Technol. 19 (2021) 811–829.
[27] L.R.Van Loon, M.A. Glaus, S. Stallone, A. Laube, in: Alkaline Degradation of Cellulose: Estimation of the Concentration of Isosaccharinic Acid in Cement Porewater 506, MRS Online Proceedings Library, 1997, pp. 1009–1010.
[28] M.A. Glaus, L.R. van Loon, S. Achatz, A. Chodura, K. Fischer, Degradation of cellulosic materials under the alkaline conditions of a cementitious repository for low and intermediate level radioactive waste part I: identification of degradation products, Anal. Chim. Acta 398 (1999) 111–122.
[29] W. Hummel, G. Anderegg, L. Rao, I. Puigdomenech, O. Tochiyama, Chemical Thermodynamics of Compounds and Complexes of U, Np, Pu, Am, Tc, Se, Ni and Zr With Selected Organic Ligands, Elsevier, North-Holland, Amsterdam, 2005.
[30] X. Gaona, V. Montoya, E. Colas, M. Grive, L. Duro, Review of the complexation of tetravalent actinides by ISA and gluconate under alkaline to hyperalkaline conditions, J. Contam. Hydrol. 102 (2008) 217–227.
[31] D. Rai, A. Kitamura, Thermodynamic equilibrium constants for important isosaccharinate reactions: a review, J. Chem. Thermodyn. 114 (2017) 135–143.
[32] J. Tits, E. Wieland, M.H. Bradbury, The effect of isosaccharinic acid and gluconic acid on the retention of Eu(III), Am(III) and Th(IV) by calcite, Appl. Geochem. 20 (2005) 2082–2096.
[33] M.R. González-Siso, X. Gaona, L. Duro, M. Altmaier, J. Bruno, Thermodynamic model of Ni(II) solubility, hydrolysis and complex formation with ISA, Radiochim. Acta 106 (2018) 31–45.
[34] T. Kobayashi, T. Teshima, T. Sasaki, A. Kitamura, Thermodynamic model for Zr solubility in the presence of gluconic acid and isosaccharinic acid, J. Nucl. Sci. Technol. 54 (2017) 233–241.
[35] K. Vercammen, M.A. Glaus, L.R.V. Loon, Complexation of Th(IV) and Eu(III) by α-isosaccharinic acid under alkaline conditions, Radiochim. Acta 89 (2001) 393–402.
[36] A. Tasi, Solubility, Redox and Sorption Behavior of Plutonium in the Presence of α-D-Isosaccharinic Acid and Cement Under Reducing Conditions, 2018. PhD Thesis.
[37] A. Tasi, X. Gaona, D. Fellhauer, M. Bottle, J. Rothe, K. Dardenne, R. Polly, M. Grivé, E. Colàs, J. Bruno, K. Kallstrom, M. Altmaier, H. Geckeis, Thermodynamic description of the plutonium – α–d–isosaccharinic acid system ii: formation of quaternary Ca(II)–Pu(IV)–OH–ISA complexes, Appl. Geochem. 98 (2018) 351–366.
[38] M. Keith-Roach, M. Lindgren, K. Kallstrom, Assessment of Complexing Agent Concentrations in SFR, 2014.
[39] L.R. Van Loon, M.A. Glaus, S. Stallone, A. Laube, Sorption of isosaccharinic acid, a cellulose degradation product, on cement, Environ. Sci. Technol. 31 (1997) 1243–1245.
[40] I. Pointeau, N. Coreau, P.E. Reiller, Uptake of anionic radionuclides onto degraded cement pastes and competing effect of organic ligands, Radiochim. Acta 96 (2008) 367–374.
[41] D. García, P. Henocq, O. Riba, M. López-García, B. Madé, J.-C. Robinet, Adsorption behaviour of isosaccharinic acid onto cementitious materials, Appl. Geochem. 118 (2020), 104625.
[42] A. Tasi, X. Gaona, T. Rabung, D. Fellhauer, J. Rothe, K. Dardenne, J. Lutzenkirchen, M. Grive, E. Colas, J. Bruno, K. Kallstrom, M. Altmaier, H. Geckeis, Plutonium retention in the isosaccharinate - cement system, Appl. Geochem. 126 (2021).
[43] M.A. Glaus, A. Laube, L.R. Van Loon, Solid–liquid distribution of selected concrete admixtures in hardened cement pastes, Waste Manag. 26 (2006) 741–751.
[44] G. Qiao, D. Hou, P. Wang, Z. Lu, Insights on failure modes of calcium-silicate-hydrate interface strengthened by polyacrylamides: structure, dynamic and mechanical properties, Constr. Build. Mater. 278 (2021), 122406.
[45] N.K. Ilango, P. Gujar, A.K. Nagesh, A. Alex, P. Ghosh, Interfacial adhesion mechanism between organic polymer coating and hydrating cement paste, Cem. Concr. Compos. 115 (2021), 103856.
[46] S. Zhang, E. Duque-Redondo, A. Kostiuchenko, J.S. Dolado, G. Ye, Molecular dynamics and experimental study on the adhesion mechanism of polyvinyl alcohol (PVA) fiber in alkali-activated slag/fly ash, Cem. Concr. Res. 145 (2021), 106452.
[47] T. Jamil, A. Javadi, H. Heinz, Mechanism of molecular interaction of acrylate-polyethylene glycol acrylate copolymers with calcium silicate hydrate surfaces, Green Chem. 22 (2020) 1577–1593.
[48] I. Androniuk, C. Landesman, P. Henocq, A.G. Kalinichev, Adsorption of gluconate and uranyl on C-S-H phases: combination of wet chemistry experiments and

molecular dynamics simulations for the binary systems, Phys. Chem. Earth A/B/C 99 (2017) 194–203.
[49] O. Chaudhari, J.J. Biernacki, S. Northrup, Effect of carboxylic and hydroxycarboxylic acids on cement hydration: experimental and molecular modeling study, J. Mater. Sci. 52 (2017) 13719–13735.
[50] N. Cevirim-Papaioannou, Y. Jo, K. Franke, M. Fuss, B.d. Blochouse, M. Altmaier, X. Gaona, Uptake of niobium by cement systems relevant for nuclear waste disposal: Impact of ISA and chloride, Cem. Concr. Res. 153 (2022) 106690.
[51] C. Cachoir, P.D. Canniere, F. Druyts, K. Ferrand, B. Kursten, K. Lemmens, T. Mennecart, E. Valcke, in: Preparation of Evolved Cement Water (ECW) and Young Cement Waters (YCW and YCWCa) for the Supercontainer Experiments, IW. W&D.0088, 2006, pp. 1–9.
[52] E. Giffaut, M. Grivé, P. Blanc, P. Vieillard, E. Colàs, H. Gailhanou, S. Gaboreau, N. Marty, B. Madé, L. Duro, Andra thermodynamic database for performance assessment: ThermoChimie, Appl. Geochem. 49 (2014) 225–236.
[53] X. Cong, R.J. Kirkpatrick, 29Si MAS NMR study of the structure of calcium silicate hydrate, Adv. Cem. Based Mater. 3 (1996) 144–156.
[54] C. Roosz, P. Vieillard, P. Blanc, S. Gaboreau, H. Gailhanou, D. Braithwaite, V. Montouillout, R. Denoyel, P. Henocq, B. Madé, Thermodynamic properties of C-S-H, C-A-S-H and M-S-H phases: results from direct measurements and predictive modelling, Appl. Geochem. 92 (2018) 140–156.
[55] R.J. Kirkpatrick, A.G. Kalinichev, X. Hou, L. Struble, Experimental and molecular dynamics modeling studies of interlayer swelling: water incorporation in kanemite and ASR gel, Mater. Struct. 38 (2005) 449–458.
[56] C. Dudás, B. Kutus, É. Boszorményi, G. Peintler, Z. Kele, I. Pálinkó, P. Sipos, Comparison of the Ca2+ complexing properties of isosaccharinate and gluconate – is gluconate a reliable structural and functional model of isosaccharinate? Dalton Trans. 46 (2017) 13888–13896.
[57] E.P. Nielsen, D. Herfort, M.R. Geiker, Binding of chloride and alkalis in Portland cement systems, Cem. Concr. Res. 35 (2005) 117–123.
[58] Y. Xu, The influence of sulphates on chloride binding and pore solution chemistry, Cem. Concr. Res. 27 (1997) 1841–1850.
[59] T. Luping, L.-O. Nilsson, Chloride binding capacity and binding isotherms of OPC pastes and mortars, Cem. Concr. Res. 23 (1993) 247–253.
[60] F.P. Glasser, J. Marchand, E. Samson, Durability of concrete — degradation phenomena involving detrimental chemical reactions, Cem. Concr. Res. 38 (2008) 226–246.
[61] M. Balonis, B. Lothenbach, G. Le Saout, F.P. Glasser, Impact of chloride on the mineralogy of hydrated Portland cement systems, Cem. Concr. Res. 40 (2010) 1009–1022.
[62] I. Androniuk, Effects of Cement Organic Additives on the Adsorption of Uranyl Ions on Calcium Silicate Hydrate Phases: Experimental Determination and Computational Molecular Modelling, 2017. PhD Thesis.
[63] N. Çevirim-Papaioannou, I. Androniuk, S. Han, N.A. Mouheb, S. Gaboreau, W. Um, X. Gaona, M. Altmaier, Sorption of beryllium in cementitious systems relevant for nuclear waste disposal: quantitative description and mechanistic understanding, Chemosphere 282 (2021), 131094.
[64] V. Bugris, C. Dudás, B. Kutus, V. Harmat, K. Csankó, S. Brockhauser, I. Pálinkó, P. Turner, P. Sipos, Crystal and solution structures of calcium complexes relevant to problematic waste disposal: calcium gluconate and calcium isosaccharinate, Acta Crystallogr. Sect. B 74 (2018) 598–609.
[65] P. Li, K.M. Merz, Taking into account the ion-induced dipole interaction in the nonbonded model of ions, J. Chem. Theory Comput. 10 (2014) 289–297.
[66] A.G. Kalinichev, R.J. Kirkpatrick, Molecular dynamics modeling of chloride binding to the surfaces of calcium hydroxide, hydrated calcium aluminate, and calcium silicate phases, Chem. Mater. 14 (2002) 3539–3549.
[67] T. Pan, K. Xia, L. Wang, Chloride binding to calcium silicate hydrates (C-S-H) in cement paste: a molecular dynamics analysis, Int. J. Pavement Eng. 11 (2010) 367–379.
[68] D. Hou, Z. Li, Molecular dynamics study of water and ions transport in nano-pore of layered structure: a case study of tobermorite, Microporous Mesoporous Mater. 195 (2014) 9–20.
[69] Y. Zhou, D. Hou, J. Jiang, L. Liu, W. She, J. Yu, Experimental and molecular dynamics studies on the transport and adsorption of chloride ions in the nano-pores of calcium silicate phase: the influence of calcium to silicate ratios, Microporous Mesoporous Mater. 255 (2018) 23–35.
[70] D. Hou, T. Li, P. Wang, Molecular dynamics study on the structure and dynamics of NaCl solution transport in the nanometer channel of CASH gel, ACS Sustain. Chem. Eng. 6 (2018) 9498–9509.
[71] I.-H. Svenum, I.G. Ringdalen, F.L. Bleken, J. Friis, D. Hoche, O. Swang, Structure, hydration, and chloride ingress in C-S-H: insight from DFT calculations, Cem. Concr. Res. 129 (2020), 105965.